Electromechanical properties in CaTiO$_3$ modified Na$_{0.5}$Bi$_{0.5}$TiO$_3$-BaTiO$_3$ solid solutions above morphotropic phase boundary

M. Jurjans ; L. Bikse ; E. Birks ; Š. Svirskas ; M. Antonova; M. Kundzins ✉ ; A. Sternberg

Check for updates

CrossMark

View Online   Export Citation

Articles You May Be Interested In

Structure and dielectric properties of Na$_{0.5}$Bi$_{0.5}$TiO$_3$-CaTiO$_3$ solid solutions

J. Appl. Phys. (February 2016)

Presence of a monoclinic (Cc) phase in the (1−x)BiFeO$_3$-xCaTiO$_3$ solid solution nanoparticles: A Rietveld study

J. Appl. Phys. (November 2017)

An indirectly coupled open-ended resonator applied to characterize dielectric properties of MgTiO$_3$–CaTiO$_3$ powders

J. Appl. Phys. (May 2014)
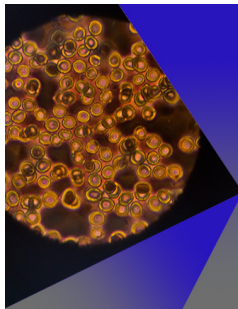
Electromechanical properties in CaTiO₃ modified Na$_{0.5}$Bi$_{0.5}$TiO$_3$-BaTiO$_3$ solid solutions above morphotropic phase boundary

View Online   Export Citation   CrossMark

M. Jurjans,[1] [ID] L. Bikse,[1] [ID] E. Birks,[1] [ID] Š. Svirskas,[2] [ID] M. Antonova,[1] M. Kundzins,[1,a)] [ID] and A. Sternberg[1] [ID]

AFFILIATIONS

[1] Institute of Solid State Physics, University of Latvia, Riga LV-1063, Latvia
[2] Faculty of Physics, Vilnius University, Vilnius LT-10222, Lithuania

[a)] Author to whom correspondence should be addressed: Maris.Kundzins@cfi.lu.lv

ABSTRACT

The structural, electromechanical, and dielectric properties of $(1 - x)(0.8Na_{0.5}Bi_{0.5}TiO_3\text{-}0.2BaTiO_3)\text{-}xCaTiO_3$ $[(1 - x)\,(0.8NBT\text{-}0.2BT)\text{-}xCT]$ ceramics are studied as candidates for room temperature actuators with high field-induced strain. The choice of 0.8NBT-0.2BT as a starting composition is motivated by the large tetragonality in this concentration range, even though it is located far away from the morphotropic phase boundary. CaTiO$_3$ was chosen as a third component to decrease the depolarization temperature and achieve a high field-induced strain at room temperature. The measured strains at the field-induced phase transition are remarkably lower than might be expected from the jump in unit cell parameters at the phase transition. This inconsistency could be related to an incomplete field-induced phase transition from the ferroelectric phase to the nonpolar phase. Among all of the manufactured samples, the phase transition is close to room temperature in the composition with x = 0.100, which allows obtaining unipolar strains up to 0.23% at E = 65 kV/cm. Electrostrictive-like strain was observed not only above the depolarization temperature but also in the region of field-induced phase transition.

I. INTRODUCTION

Na$_{0.5}$Bi$_{0.5}$TiO$_3$ (NBT) based compositions are widely studied due to environmental requirements, which necessitate the replacement of lead-containing ferroelectrics in a large variety of devices applying the piezoelectric effect. NBT-based compositions have already shown useful properties, such as large field-induced strain,[1] high stored electric energy density,[2] and excellent mechanical quality factor at high ultrasonic power.[3]

In lead-containing ferroelectric solid solutions, the highest piezoelectric coefficients are found in the region of the morphotropic phase boundary (MPB) between ferroelectric phases possessing different symmetries.[4] Such an approach was also applied in the case of solid NBT-based solutions, focusing on the rhombohedral–tetragonal MPB in Na$_{0.5}$Bi$_{0.5}$TiO$_3$–BaTiO$_3$ (NBT–BT)[5] and Na$_{0.5}$Bi$_{0.5}$TiO$_3$–K$_{0.5}$Bi$_{0.5}$TiO$_3$ (NBT–KBT)[6] solid solutions. Indeed, the piezoelectric coefficient increased upon approaching the MPB, although the increase was moderate and did

not immediately attract great practical interest. Besides, approaching the MPB is accompanied by the reduction of the depolarization temperature (T_d), which usually is disadvantageous. At the same time, in the temperature region of T_d, double hysteresis loops are observed together with large field-induced strain, corresponding to the phase transition between the antiferroelectric and ferroelectric states.[7] Such features inspired the idea to reduce T_d even further by using an appropriate modification of compositions at MPB, achieving the field-induced phase transition strain within the room temperature range. Indeed, in the case of NBT-BT solid solutions, such modification was realized with various modifiers, for example, K$_{0.5}$Na$_{0.5}$NbO$_3$ (KNN).[8] 2 mol. % of KNN in 0.92NBT-0.06BT-0.02KNN composition was sufficient to shift T_d into the room temperature range and achieve high strain values reaching 0.46% at E = 80 kV/cm. Thereafter, a decrease in the depolarization temperature in various NBT-based solid solutions and shifting of the field-induced phase transition to the room temperature range

were reported, enabling strains at even above 0.6%.[1,9,10] At the same time, it can be observed that the modification of the initial composition, which is aimed at reducing T_d, simultaneously reduces the maximum value of strain observed in the T_d region.[11–13] Strictly speaking, MPB, in this case, has a different meaning compared to how it was previously introduced in the Pb-based solid solutions, especially $Pb(Zr,Sn,Ti)O_3$. First, in the NBT-based solid solutions, it is a boundary between the ferroelectric and nonpolar states, and the relationship with the rhombohedral–tetragonal phase boundary, observed in the unmodified compositions such as 0.94NBT-0.06BT and 0.84NBT-0.16KBT, is not quite clear, except for an indirect role—T_d reaches a minimum at the MPB.[5,6] Second, such MPB has a pronounced temperature dependence.

The reasons for high strain at MPB in the NBT-based solid solutions have been repeatedly discussed. In the case of NBT-BT, taking into account the observed double hysteresis loops, large strains initially were explained by a field-induced phase transition between the antiferroelectric and ferroelectric phases,[7] assuming a similarity with well-known $Pb(Zr,Sn,Ti)O_3$ ternary solutions.[14] Later, taking into account the characteristics of relaxor state dielectric dispersion in the NBT-based compositions, T_d was interpreted as a phase transition temperature between the ergodic and non-ergodic relaxor states.[15,16] In the presence of an electric field, the phase transition from the relaxor to ferroelectric state takes place,[17,18] which leads to double hysteresis loops and the jump of field induced strain. Moreover, careful analysis of different contributions to strain at room temperature (intrinsic or lattice strain, strain due to domain switching, and strain of phase transition) revealed that the strain of a field-induced phase transition (not involving an anti-ferroelectric phase) is important, but not a major contributor toward total strain.[19] It can also be seen that the simultaneous presence of different ferroelectric phases with different behaviors when placed in an electric field makes the comprehensive analysis quite complicated.

The concept of the role played by the anti-ferroelectric phase was extended also to NBT-BT-KNN solid solutions.[8] Later, low values of volume strain (ΔV_{PT}) at the field-induced phase transition led to explain large values of strain by the non-180° reorientation of domains.[20] Indeed, domain reorientations should not influence a volume change, although it is still not clear why a small volume jump at the phase transition is a reason to reject the dominating contribution of the phase transition jump with linear strain. In ceramics, volume change as a factor of polarization is determined by the volume electrostriction coefficient $Q_v = Q_{33} + 2Q_{12}$, where Q_{33} is the electrostriction coefficient along the direction of the electric field and Q_{12} is aligned in the perpendicular direction. Negative Q_{12} is frequently observed in ferroelectrics, but in the case of relaxor ferroelectrics, the absolute value of Q_{12} is large enough compared with Q_{33} to remarkably reduce Q_v.[21] During the phase transition between the centrosymmetric nonpolar and ferroelectric phases, the volume jump at the phase transition is determined by $\Delta V_{PT} = Q_v \cdot P_s^2$. If it is valid also for relaxor ferroelectrics, the volume jump at the phase transition will be small, despite remarkable jumps in the linear strains u_{33} and u_{12}.

Considering that the main reason for large strains is the phase transition between the nonpolar and polar states, restricting the solid solution concentration range to MPB does not look convincing, and the search for large field-induced strains can be extended outside MPB, using appropriate criteria. Dunce et al.[22] showed that, among NBT-BT solid solutions, a composition of 0.8NBT-0.2BT has a high tetragonality of the unit cell (c/a − 1 = 0.020). Unlike with the compositions close to MPB, at this part in the NBT-BT phase diagram, a rhombohedral phase is not involved, and the phase transition (in regard to the lattice symmetry) is much simpler, involving only macroscopic nonpolar and tetragonal phases. Thus, 0.8NBT-0.2BT can be selected as the starting composition as tetragonality, especially close to T_d, should be directly related to accessible strain. Therefore, it is reasonable to consider the modification of this composition to reduce T_d, trying to maintain enough high tetragonality.

In this work, $CaTiO_3$ is chosen as a third component for 0.8NBT-0.2BT solid solution, and compositions (1 − x)(0.8NBT-0.2BT)-xCT with x = 0, 0.05, 0.075, 0.100, and 0.125 are prepared via the solid–state reaction method. The effects of $CaTiO_3$ dopant on the crystalline structure, microstructure, electromechanical, and dielectric properties are studied.

II. EXPERIMENTAL PROCEDURE

A. Sample preparation

(1 − x)($0.8Na_{0.5}Bi_{0.5}TiO_3$-$0.2BaTiO_3$)-$xCaTiO_3$ ceramics with various CT concentrations from x = 0 to x = 0.125 were prepared by solid state reaction from chemical-grade oxides and carbonates. The two-stage calcination was performed at temperatures 850 and 1000 °C and sintering at 1140–1200 °C depending on the composition.

B. Measurements

The crystal structures of the crushed ceramic samples were determined using an x-ray diffractometer *PANalytical X'Pert PRO*. Lattice symmetry and unit cell parameters were obtained, treating diffraction patterns by Rietveld analysis. The morphology of the thermally etched sample surface was analyzed using scanning electron microscopy (*Lyra, Tescan*). To test the electromechanical properties, the sintered samples were polished to 0.3 mm thickness. The electrodes were made by firing gold paste at 500 °C. The macroscopic strain measurements were carried out using a linear variable displacement transducer (LVDT) (*Tesa TT-90*). The sample was placed in a special container filled with oil to prevent dielectric breakdown and suitable for heating to perform experiments at various temperatures. The polarization hysteresis (P-E) loops were measured simultaneously with strain dependence on the electric field using the Sawyer–Tower method. Both measurements at the bipolar and unipolar pulses were made at 12.5 mHz frequency. The dielectric properties were measured using *HP precision LCR meter 4284A* at frequencies from 100 Hz to 1 MHz upon heating the previously poled samples. The piezoelectric constant d_{33} of samples, poled at room temperature, was measured using *YE2730A* d_{33} meter.

In the measurements of a field-induced strain, the asymmetric strain loops are repeatedly presented,[23,24] which, from our point of view, is hard to explain, taking into account that the polarization hysteresis loops look symmetric. Such an asymmetry was also observed in this work if the samples were placed on a flat surface. However, the asymmetry was eliminated using a quasi-spherical bottom surface, which remarkably limits the area where the sample

touches a surface. This finding hints that the asymmetry is created by arbitrary bending of the sample due to the nonhomogeneous distribution of strain, especially close to the edges of the sample, and does not represent a real change in the sample dimension in the direction of the electric field.

III. RESULTS AND DISCUSSION

X-ray diffraction patterns of $(1 - x)(0.8NBT\text{-}0.2BT)\text{-}xCT$ at low concentrations of $CaTiO_3$ reveal a clear splitting of diffraction maxima that is sensitive to tetragonal distortion. Upon increasing the $CaTiO_3$ concentration, the splitting steeply reduces and disappears at around x = 0.075 (Figs. 1 and 2), revealing the phase boundary between the phases of tetragonal and cubic symmetry at room temperature. The unit cell parameter *c* reduces remarkably upon increasing $CaTiO_3$ content while *a* increases, but to a much less extent.

Comparing the poled and virgin (unpoled) samples (Fig. 2), a slight increase of unit cell parameter *c* and decrease of *a* are observed, which is also reflected in tetragonality—it is larger for the poled samples (values of tetragonality for the poled samples are given in Table I). The virgin composition with x = 0.075 is of cubic symmetry, while the electric field can irreversibly induce a phase of tetragonal symmetry at room temperature. For composition with x = 0.05, which is in a ferroelectric state at room temperature, the unit cell parameter *c* decreases and *a* increases upon increasing the temperature (see Fig. 3) until it reaches a phase coexistence region. In this region, the coexistence of phases with tetragonal and cubic symmetry, as well as a larger jump in value for the unit cell parameter *c* and a smaller one for *a*, is observed, which is characteristic for the first order phase transition. For the unpoled composition with x = 0.075, the unit cell parameter linearly increases upon
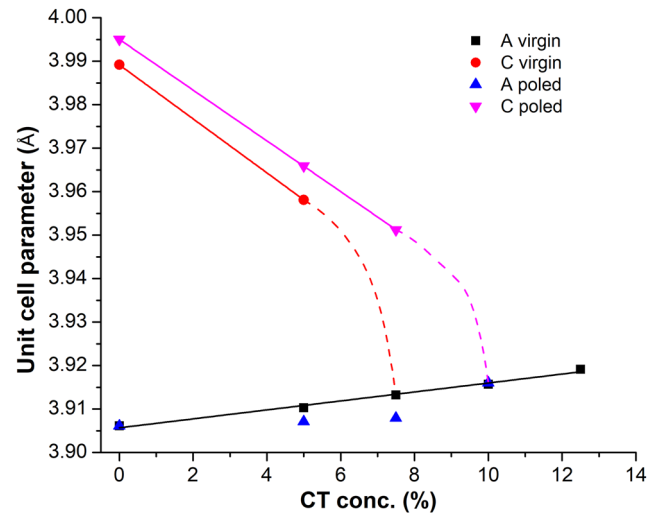
FIG. 2. Concentration dependence of lattice parameters for the virgin and poled samples of $(1 - x)(0.8NBT\text{-}0.2BT)\text{-}xCT$ solid solutions at room temperature.

increasing the temperature. The temperature dependence of the dielectric permittivity of poled samples upon heating (Fig. 4) allows evaluating the depolarization temperature. It can be clearly identified for compositions with $CaTiO_3$ concentration up to 5 mol. %, where the maximum of $\varepsilon''(T)$ corresponds to the steepest change in $\varepsilon'(T)$. For compositions with a higher concentration of $CaTiO_3$, the maximum of $\varepsilon''(T)$ is independent of x and therefore cannot be related to the depolarization temperature. At the same time, the composition with x = 0.075 has a stable remnant polarization at
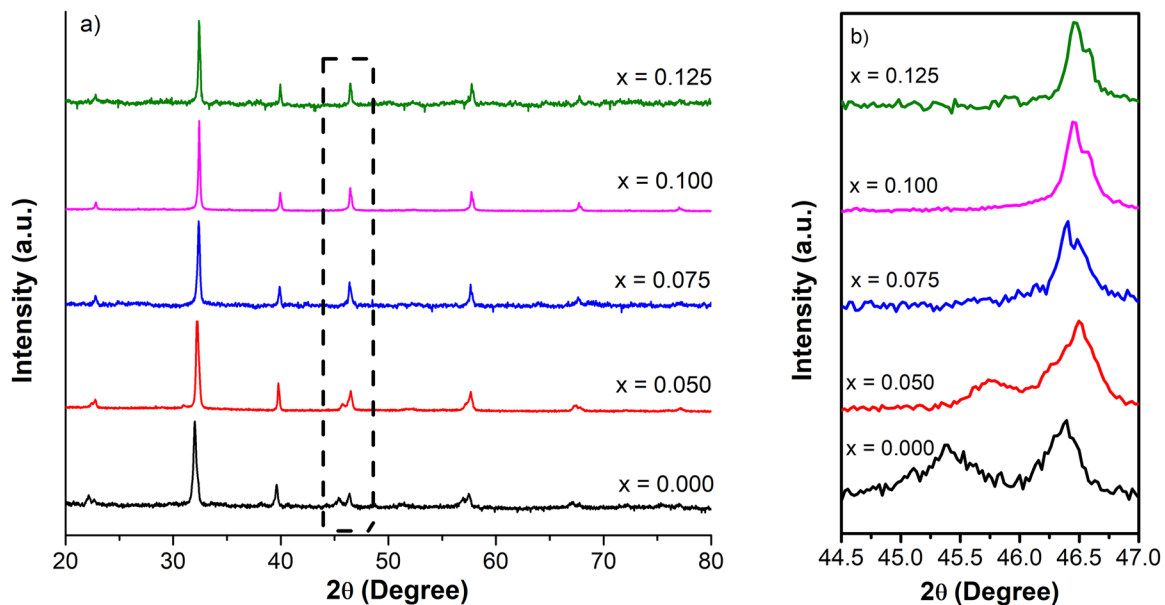
FIG. 1. (a) X-ray diffraction patterns at room temperature for all $(1 - x)(0.8NBT\text{-}0.2BT)\text{-}xCT$ compositions and (b) enlarged view of pseudocubic [200] maximum.

TABLE I. Impact of CaTiO$_3$ on tetragonality (c/a) for the poled samples, maximal polarization (P$_{max}$), piezoelectric coefficient (d$_{33}$), electrostriction coefficient (Q$_{33}$) at room temperature, and depolarization temperature (T$_d$).

CaTiO$_3$	0.000	0.050	0.075	0.100	0.125
c/a	1.022 75	1.012 22	1.011 08	$\cdots$	$\cdots$
P$_{max}$ (μC/cm^2)	30.3	34.0	25.9	24.9	24.6
d$_{33}$	106	100	112	$\cdots$	$\cdots$
Q$_{33}$ (m^4/C^2)	$\cdots$	0.027[a]	0.032[b]	0.033	0.028
T$_d$ ($^\circ$C)	202	115	53	$\cdots$	$\cdots$

[a]This value was obtained at 130 °C.
[b]This value was obtained at 70 °C.

room temperature, which upon heating has the steepest reduction in 50–60 °C temperature range [corresponds to the steepest increase in induced polarization in Fig. 7(b)]. Apparently, in the temperature dependence of ε''(T), the maximum (which is related to T$_d$) is disguised by contributions that are not related to depolarization. At the same time, ε'(T) still contains a part of a steep change, which can be related to T$_d$. The depolarization temperatures of compositions with x ≤ 0.075 are presented in Table I.

The polarization hysteresis P(E) loops for the samples of all compositions at room temperature are shown in Fig. 5. The compositions with low content of CaTiO$_3$ (x ≤ 0.075) have well-expressed ferroelectric hysteresis loops with a small difference between the maximal and remnant polarization. At x = 0.100, the P(E) loop transforms to a double hysteresis loop, which is characteristic of the first order phase transition, while for the composition with x = 0.125, the features of a double hysteresis loop almost vanish. P(E) gets slimmer and more pinched upon increasing x, where x > 0.050. Since the critical electric field (E$_c$) for the phase transition from the ferroelectric to nonpolar phase for the composition with x = 0.100 is positive, it can be concluded that T$_d$ approaches room temperature (E$_c$ = 0) in CaTiO$_3$ concentration range between 0.075 and 0.100.

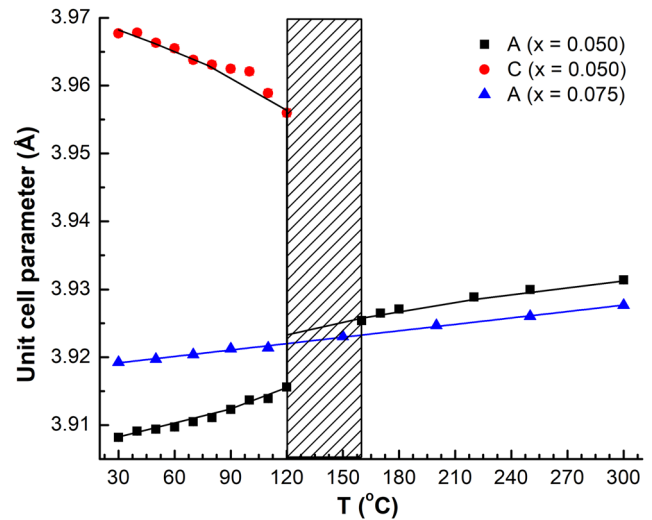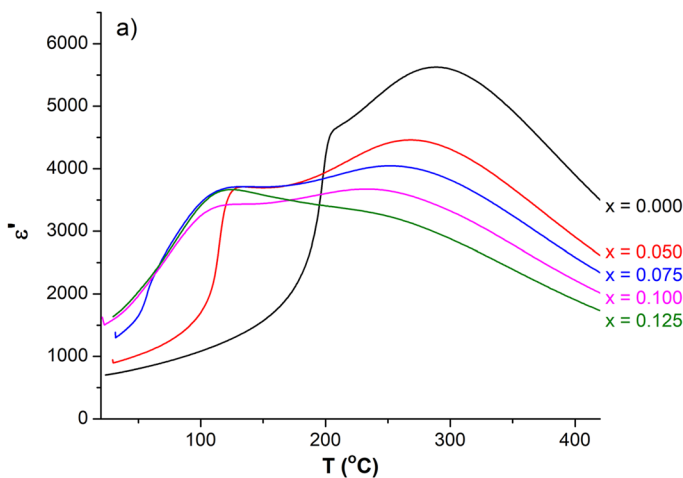**FIG. 3.** Temperature dependence of lattice parameters for the poled sample of composition with x = 0.050 and the unpoled sample of composition with x = 0.075. The data are collected upon heating.

The composition with x = 0.050 has the largest polarization at room temperature. The increase of polarization in this composition, in comparison with the composition with x = 0, at least partly can be explained by the reduction of coercive field (E$_{coerc}$) and consequently more complete polarization reversal in bipolar field cycle. The remnant polarization has a remarkable drop in the CaTiO$_3$ concentration range between 0.075 and 0.100.

Strain response to a bipolar electric field pulse is shown in Fig. 6(a). For ceramics with x = 0, 0.05, and 0.075 strain vs electric field has a typical butterfly-shape, while for compositions with x = 0.100 and 0.125, negative strain vanishes, which is a characteristic strain response for relaxor ferroelectric materials. At room
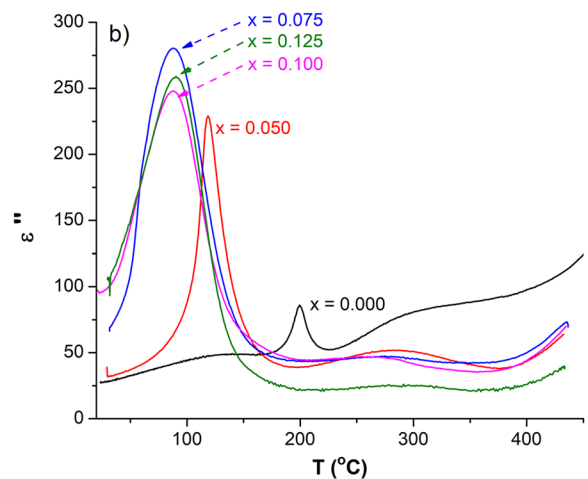

FIG. 4. Temperature dependence of the real (a) and imaginary (b) parts of dielectric permittivity, measured on heating at 1 kHz of the poled (1 − x)(0.8NBT-0.2BT)-xCT samples.

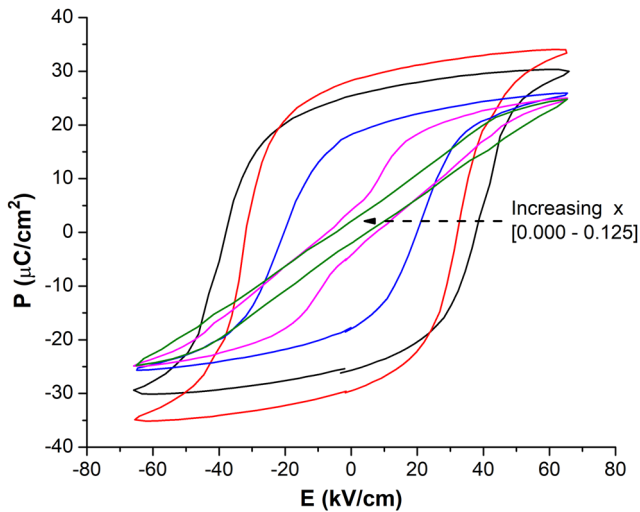**FIG. 5.** P-E hysteresis loops of $(1 - x)(0.8NBT-0.2BT)-xCT$ samples at room temperature.

temperature, the highest strain (0.23%) is achieved for x = 0.100 because of the electric field-induced phase transition. Unipolar strain maxima at room temperature [Fig. 6(b)] show similar dependence on $CaTiO_3$ concentration as for bipolar pulses.

The temperature dependence of strain (u_{max}) and induced polarization (P_{i-max}) at the maximal value of unipolar field pulses ($E_{max} = 65$ kV/cm) is presented in Fig. 7. In the sample with x = 0, T_d is at 202 °C and therefore exhibits only a slight increase in induced polarization and strain in the measured temperature interval. For samples with x = 0.050 and 0.075, a strong increase in P_{i-max} is observed upon approaching T_d, which results in a steep increase in unipolar strain, especially for the composition with x = 0.05, reaching 0.32% in the region of T_d. For samples with x = 0.100 and 0.125,

induced polarization has weak temperature dependence, while the unipolar strain decreases with the increase of temperature.

It is interesting to compare the directly measured values of strain in the temperature range of field induced-phase transition and the jump of unit cell parameters at the phase transition. Due to the different orientations of crystallographic axes in different grains, the strain should be averaged across these directions. As a result, a jump contribution in strain from the field-induced phase transition should be lower compared to the jump in unit cell parameters, especially in the case of a large, negative Δa.

For the composition with x = 0.05, a comparison can be done using XRD data presented in Fig. 3. The temperature range where u(T) reaches maximal values is close to the lowest temperature of the phase coexistence region, determined from the XRD measurements. The corresponding value of c of the ferroelectric state and that extrapolated to the same temperature value of c of the nonpolar phase gives a jump of $\Delta c = 0.83\%$. Similarly, a jump of unit cell parameter a can be obtained: $\Delta a = -0.20\%$. Taking into account that the directly measured strain [u(max) = 0.32%] contains other contributions, besides the jump at the phase transition, it should be considered as rather low.

In the case of x = 0.075, another approach is reasonable to apply. The difference in the values of unit cell parameters between the virgin and poled samples at room temperature is $\Delta c = 0.97\%$ and $\Delta a = -0.05\%$. This difference can be compared to the strain that remains after the unipolar field pulse is applied for the first time to a virgin sample (u_{rem}). Unlike in the previous case, this value does not contain any other contributions except a field-induced phase transition. The obtained value of strain, $u_{rem} = 0.075\%$, compared to the jump in lattice parameters is too low to only be explained by the different orientations of crystallographic axes in different grains. The reason for low u_{rem} could be random lattice strains due to the presence of spatially nonhomogeneous polarization such as polar nanoregions in a nonpolar, virgin state, which are eliminated after the transition to the ferroelectric state. This situation is very different from compositions at the MPB, where the contribution from a jump in
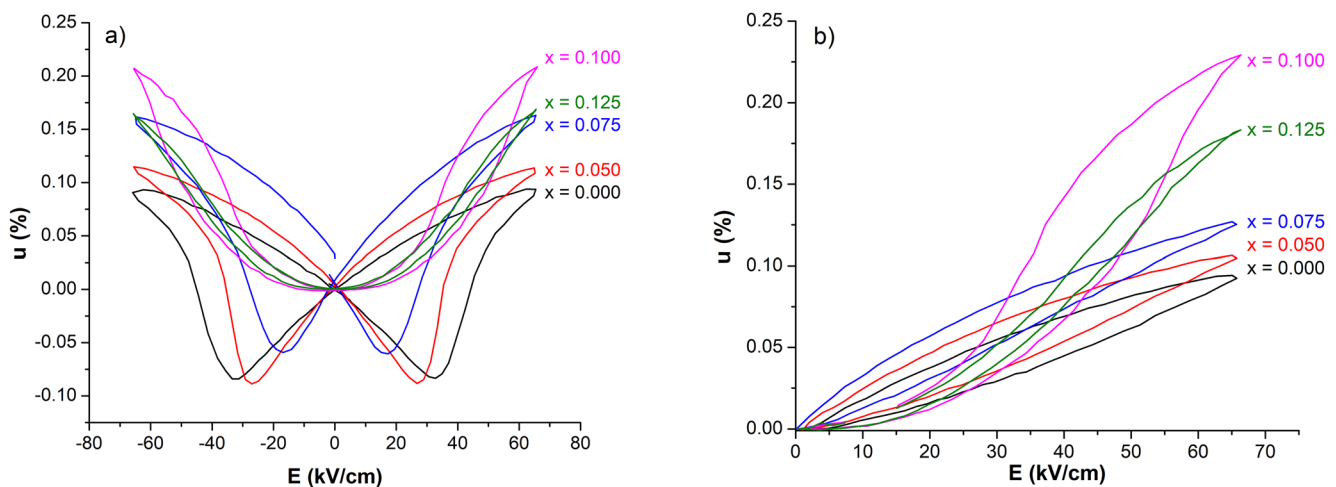

FIG. 6. (a) Bipolar and (b) unipolar strain loops of $(1 - x)(0.8NBT-0.2BT)-xCT$ samples at room temperature.

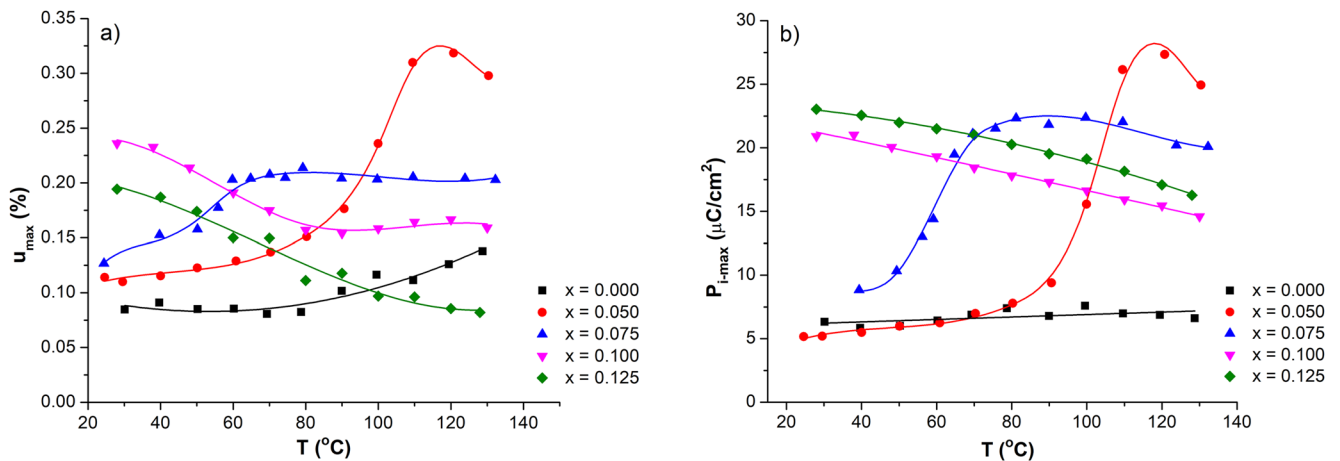**FIG. 7.** (a) Maximal unipolar strain and (b) induced polarization vs temperature for $(1 - x)(0.8NBT-0.2BT)-xCT$ samples at $E = 65$ kV/cm.

lattice parameters at the phase transition is remarkably lower than the measured strain.[19]

Δc was also calculated for the composition with x = 0. The obtained value of Δc = 0.81% is in the same range as for the compositions with x = 0.05 and x = 0.075, even considering that the latter was obtained below T_d. This means that the decrease of Δc at room temperature by increasing x is first related to the temperature dependence Δc(T) upon approaching T_d and reduction of temperature interval between T_d and room temperature if the concentration of $CaTiO_3$ is increased.

For ceramics with x = 0.100 and 0.125 in the whole temperature range that was studied, electrostrictive-like behavior is observed [Fig. 8(a)]: the strain vs polarization dependence corresponds to u ~ P^2 [Fig. 8(b)]. The electrostrictive coefficients Q_{33} for x = 0.100

and 0.125 are 0.033 and 0.020 m^4/C^2, respectively (Table I). The origin of this phenomenon in relaxor ferroelectric materials (unlike in a purely paraelectric state) is not well understood, yet it shows a promising trend—the strain can be heavily enhanced with higher polarization. Sometimes, the compositions with larger values of Q_{33} are considered more appropriate for practical application in actuators.[25] However, more important for a practical application are the values of strain and the corresponding electric field,[26] even considering that strains' dependence on the electric field cannot be characterized by a single parameter, such as Q_{33}. For example, a strain value of u = 0.2%, obtained in the present study with x = 0.100 at 65 kV/cm, while for PMN-PT, the same strain is obtained at 20 kV/cm.[27] At the same time, the electrostriction coefficient for the composition with x = 0.100 is even higher. The reason for lower
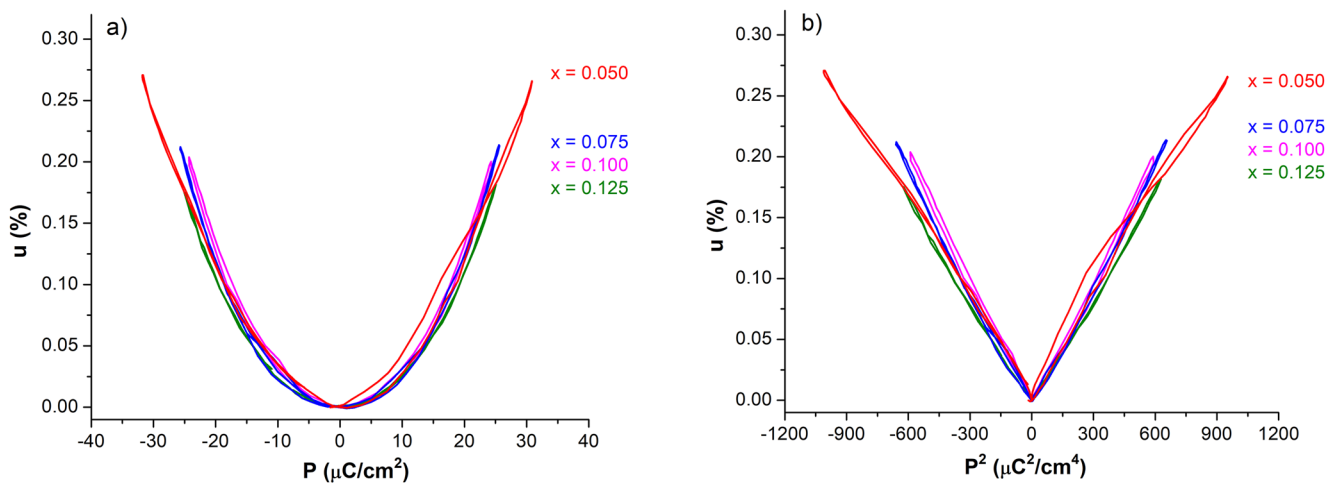

FIG. 8. (a) Strain vs polarization and (b) polarization squared for various $(1 - x)(0.8NBT-0.2BT)-xCT$ compositions at temperatures 130 °C (x = 0.050), 70 °C (x = 0.075), 23 °C (x = 0.100), and 23 °C (x = 0.125).

strain in the case of x = 0.100 and NBT-based compositions, in general, is lower field-induced polarization.

The observation of electrostrictive character for strain at the field-induced phase transition in compositions with x = 0.050, 0.075, and 0.100 attracts special interest because they are observed not only above T_d but also in the region of the first order field-induced phase transition. Such dependence, observed also in Refs. 28 and 29, suggests a continuous change of polarization between P = 0 and P_{max} simultaneously throughout a sample, instead of the usually accepted phase transformation mechanism at the first order phase transition, where the concentration of one phase increases at the expense of the other phase. It also means that the mechanism determining the dependence of strain on polarization is the same both in a non-polar state and phase transition. Therefore, the phase transition strain, in this case, should be considered not as an extrinsic mechanism[19] but an intrinsic one. Such behavior of u(P) resembles the character of strain as a factor of polarization at the ferroelectric-centrosymmetric paraelectric phase transition, where spontaneous strain at the phase transition is determined by the same electrostriction mechanism valid for both the paraelectric and ferroelectric states.

The impact of $CaTiO_3$ on various properties is summarized in Table I. A relatively sharp fall in tetragonality can be seen with the increase of the dopant concentration, while the maximal polarization does not correlate with this parameter. The piezoelectric coefficient d_{33} was also measured for the poled samples at room temperature. The changes in d_{33} upon increasing x are insignificant.

IV. CONCLUSION

The addition of $CaTiO_3$ to $0.8Na_{0.5}Bi_{0.5}TiO_3$-$0.2BaTiO_3$ solid solution, which has a large jump of the unit cell parameter c at the phase transition between the ferroelectric and nonpolar phases at T_d, allows one to reduce T_d to room temperature across the $CaTiO_3$ concentration range between 0.075 and 0.100. Despite the large jump in the unit cell parameter, maintained also in $CaTiO_3$-containing compositions, the obtained macroscopic strains do not exceed 0.32% at 65 kV/cm, which can be explained by random strains in the nonpolar phase created by polar nanoregions. Electrostriction-like behavior is observed not only above T_d, but also in the range of field-induced first order phase transition, which urges researchers to reconsider the phase transition mechanism in the studied compositions. Despite the moderate values of macroscopic strain, the large jump in the unit cell parameters at the field-induced phase transition indicates that it is worthwhile to look for compositions outside the morphotropic phase boundary for good electromechanical properties.

AUTHOR DECLARATIONS

Conflict of Interest

The authors declare no conflict of interest.

DATA AVAILABILITY

The data that support the findings of this study are available from the corresponding author upon reasonable request.

REFERENCES

[1] J. Chen, Y. Wang, L. Wu, Q. Hu, and Y. Yang, "Effect of nanocrystalline structures on the large strain of $LiNbO_3$ doped $(Bi_{0.5}Na_{0.5})TiO_3$-$BaTiO_3$ materials," J. Alloys Compd. **775**, 865–871 (2019).

[2] F. Gao, X. Dong, C. Mao, W. Liu, H. Zhang, L. Yang, F. Cao, and G. Wang, "Energy-storage properties of $0.89Bi_{0.5}Na_{0.5}TiO_3$–$0.06BaTiO_3$–$0.05K_{0.5}Na_{0.5}NbO_3$ lead-free anti-ferroelectric ceramics," J. Am. Ceram. Soc. **94**, 4382–4386 (2011).

[3] M. Hejazi, E. Taghaddos, E. Gurdal, K. Uchino, and A. Safari, "High power performance of manganese-doped BNT-based Pb-free piezoelectric ceramics," J. Am. Ceram. Soc. **97**, 3192–3196 (2014).

[4] B. Noheda, D. Cox, G. Shirane, R. Guo, B. Jones, and L. Cross, "Stability of the monoclinic phase in the ferroelectric perovskite $PbZr_{1-x}Ti_xO_3$," Phys. Rev. B **63**, 014103 (2001).

[5] M. Chen, Q. Xu, B. H. Kim, B. K. Ahn, J. H. Ko, W. J. Kang, and O. J. Nam, "Structure and electrical properties of $(Na_{0.5}Bi_{0.5})_{1-x}Ba_xTiO_3$ piezoelectric ceramics," J. Am. Ceram. Soc. **28**, 843–849 (2008).

[6] K. Yoshii, Y. Hiruma, H. Nagata, and T. Takenaka, "Electrical properties and depolarization temperature of $(Bi_{1/2}Na_{1/2})TiO_3$–$(Bi_{1/2}K_{1/2})TiO_3$ lead-free piezoelectric ceramics," Jpn. J. Appl. Phys. **45**, 4493–4496 (2006).

[7] S.-T. Zhang, A. B. Kounga, E. Aulbach, and Y. Deng, "Temperature-dependent electrical properties of $0.94Bi_{0.5}Na_{0.5}TiO_3$–$0.06BaTiO_3$ ceramics," J. Am. Ceram. Soc. **91**, 3950–3954 (2008).

[8] S.-T. Zhang, A. B. Kounga, E. Aulbach, W. Jo, T. Granzow, H. Ehrenberg, and J. Rödel, "Lead-free piezoceramics with giant strain in the system $Bi_{0.5}Na_{0.5}TiO_3$–$BaTiO_3$–$K_{0.5}Na_{0.5}NbO_3$. I. Structure and room temperature properties," J. Appl. Phys. **103**, 034108 (2008).

[9] S. Manotham, P. Jaita, C. Randorn, G. Rujijanagul, and D. P. Cann, "Excellent electric field-induced strain with high electrostrictive and energy storage performance properties observed in lead-free $Bi_{0.5}(Na_{0.84}K_{0.16})_{0.5}TiO_3$-$Ba(Nb_{0.01}Ti_{0.99})O_3$-$BiFeO_3$ ceramics," J. Alloys Compd. **808**, 151655 (2019).

[10] Q. Wei, M. Zhu, M. Zheng, and Y. Hou, "Giant strain of 0.65% obtained in B-site complex cations $(Zn_{1/3}Nb_{2/3})^{4+}$-modified BNT-7BT ceramics," J. Alloys Compd. **782**, 611–618 (2019).

[11] L. Wu, B. Shen, Q. Hu, J. Chen, Y. Wang, Y. Xia, J. Yin, and Z. Liu, "Giant electromechanical strain response in lead-free $SrTiO_3$-doped $(Bi_{0.5}Na_{0.5}TiO_3$–$BaTiO_3)$–$LiNbO_3$ piezoelectric ceramics," J. Am. Ceram. Soc. **100**, 4670–4679 (2017).

[12] N. Zhao, H. Fan, X. Ren, S. Gao, J. Ma, and Y. Shi, "A novel $((Bi_{0.5}Na_{0.5})0.94Ba_{0.06})_{1-x}(K_{0.5}Nd_{0.5})_xTiO_3$ lead-free relaxor ferroelectric ceramic with large electrostrains at wide temperature ranges," Ceram. Int. **44**, 571–579 (2018).

[13] N. Zhao, H. Fan, J. Ma, X. Ren, Y. Shi, and Y. Zhou, "Large strain of temperature insensitive in $(1 − x)(0.94Bi_{0.5}Na_{0.5}TiO_3$–$0.06BaTiO_3)$–$xSr_{0.7}La_{0.2}TiO_3$ lead-free ceramics," Ceram. Int. **44**, 11331–11339 (2018).

[14] J. Hao, W. Li, J. Zhai, and H. Chen, "Progress in high-strain perovskite piezoelectric ceramics," Mater. Sci. Eng., R **135**, 1–57 (2019).

[15] W. Jo, S. Schaab, E. Sapper, L. A. Schmitt, H.-J. Kleebe, A. J. Bell, and J. Rödel, "On the phase identity and its thermal evolution of lead free $(Bi_{1/2}Na_{1/2})TiO_3$-6 mol% $BaTiO_3$," J. Appl. Phys. **110**, 074106 (2011).

[16] L. Pardo, E. Mercadelli, A. Garcia, K. Brebol, and C. Galassi, "Field-induced phase transition and relaxor character in submicrometer-structured lead-free $(Bi_{0.5}Na_{0.5})_{0.94}Ba_{0.06}TiO_3$ piezoceramics at the morphotropic phase boundary," IEEE Trans. Ultrason., Ferroelectr., Freq. Control **58**, 1893–1904 (2011).

[17] F. Craciun, C. Galassi, and R. Birjega, "Electric-field-induced and spontaneous relaxor-ferroelectric phase transitions in $(Na_{1/2}Bi_{1/2})_{1-x}Ba_xTiO_3$," J. Appl. Phys. **112**, 124106 (2012).

[18] C. Ma, H. Guo, S. P. Beckman, and X. Tan, "Creation and destruction of morphotropic phase boundaries through electrical poling: A case study of lead-free $(Bi_{1/2}Na_{1/2})TiO_3$–$BaTiO_3$ piezoelectrics," Phys. Rev. Lett. **109**, 107602 (2012).

[19] N. H. Khansur, M. Hinterstein, Z. Wang, C. Groh, W. Jo, and J. E. Daniels, "Electric-field-induced strain contributions in morphotropic phase boundary composition of $(Bi_{1/2}Na_{1/2})TiO_3$-$BaTiO_3$ during poling," Appl. Phys. Lett. **107**, 242902 (2015).

[20] W. Jo, T. Granzow, E. Aulbach, J. Rödel, and D. Damjanovic, "Origin of the large strain response in $(K_{0.5}Na_{0.5})NbO_3$-modified $(Bi_{0.5}Na_{0.5})TiO_3$–$BaTiO_3$ lead-free piezoceramics," J. Appl. Phys. **105**, 094102 (2009).

[21] F. Li, L. Jin, Z. Xu, and S. Zhang, "Electrostrictive effect in ferroelectrics: An alternative approach to improve piezoelectricity," Appl. Phys. Rev. **1**, 011103 (2014).

[22] M. Dunce, E. Birks, M. Antonova, A. Plaude, R. Ignatans, and A. Sternberg, "Structure and dielectric properties of $Na_{1/2}Bi_{1/2}TiO_3$-$BaTiO_3$ solid solutions," Ferroelectrics **447**, 1–8 (2013).

[23] X. Liu and X. Tan, "Giant strains in non-textured $(Bi_{1/2}Na_{1/2})TiO_3$-based lead-free ceramics," Adv. Mater. **28**, 574–578 (2016).

[24] F. Li, Y. Liu, Y. Lyu, Y. Qi, Z. Yu, and C. Lu, "Huge strain and energy storage density of A-site La^{3+} donor doped $(Bi_{0.5}Na_{0.5})_{0.94}Ba_{0.06}TiO_3$ ceramics," Ceram. Int. **43**, 106–110 (2016).

[25] F.-X. Zhao, Q. He, Q.-Z. Bai, W.-J. Wu, B. Wu, and M. Chen, "Effect of Sr^{2+} on phase structure and properties for $0.6(Na_{0.5}Bi_{0.5})TiO_3$-$0.4(Bi_{1-y}Sr_y)TiO_3$ relaxor ferroelectrics," Ceram. Int. **46**, 3257–3263 (2020).

[26] T. Li, C. Liu, X. Ke, X. Liu, L. He, P. Shi, X. Ren, Y. Wang, and X. Lou, "High electrostrictive strain in lead-free relaxors near the morphotropic phase boundary," Acta Mater. **182**, 39–46 (2020).

[27] Q. Zhang, W. Pan, A. Bhalla, and L. E. Cross, "Electrostrictive and dielectric response in lead magnesium niobate–lead titanate (0.9PMN·0.1PT) and lead lanthanum zirconate titanate (PLZT 9.5/65/35) under variation of temperature and electric field," J. Am. Ceram. Soc. **72**, 599–604 (1989).

[28] Š. Svirskas, M. Dunce, E. Birks, A. Sternberg, and J. Banys, "Electromechanical properties of $Na_{0.5}Bi_{0.5}TiO_3$-$SrTiO_3$-$PbTiO_3$ solid solutions," J. Phys. Chem. Solids **114**, 94–99 (2018).

[29] J. Pang, Y. Pu, N. Xu, Y. Tian, R. Jing, D. Hongliang, X. Wei, Z. Xu, D. Guo, J. Xu, and F. Gao, "Thermally stable electrostrains and composition-dependent electrostrictive coefficient Q_{33} in lead-free ferroelectric ceramics," Ceram. Int. **45**, 22854–22861 (2019).

27 September 2023 07:05:00